Science Advances

www.advances.sciencemag.org/cgi/content/full/1/5/e1500242/DC1

Supplementary Materials for

Topological *R*PdBi half-Heusler semimetals: A new family of noncentrosymmetric magnetic superconductors

Yasuyuki Nakajima, Rongwei Hu, Kevin Kirshenbaum, Alex Hughes, Paul Syers, Xiangfeng Wang, Kefeng Wang, Renxiong Wang, Shanta R. Saha, Daniel Pratt, Jeffrey W. Lynn, Johnpierre Paglione

Published 5 June 2015, *Sci. Adv.* **1**, e1500242 (2015)
DOI: 10.1126/sciadv.1500242

This PDF file includes:

Supplementary materials for RPdBi half-Heusler semimetals: a new family of non-centrosymmetric magnetic superconductors

Y. Nakajima,[1] R. Hu,[1] K. Kirshenbaum,[1] A. Hughes,[1] P. Syers,[1] X. Wang,[1] K. Wang,[1] R. Wang,[1] S.R. Saha,[1] D. Pratt,[2] J.W. Lynn,[2] and J. Paglione[1]

[1]*Center for Nanophysics and Advanced Materials, Department of Physics, University of Maryland, College Park, MD 20742*

[2]*NIST Center for Neutron Research, National Institute of Standards and Technology, Gaithersburg, Maryland 20899*

STRUCTURAL CHARACTERIZATION

The powder X ray diffraction patterns confirm the formation of RPdBi phase with a MgAgAs-type structure (space group $F\bar{4}3m$) as shown in Fig. S1. Except for Bi flux residues, the observation of single phase of RPdBi ensures the observed magnetism and superconductivity are intrinsic. The obtained lattice parameters are close to the reported values [35] (Fig. 1 in the main text).

EXCLUSION OF POSSIBLE IMPURITY PHASES

Although X ray diffraction patterns show a single phase with small flux residues in our samples, it is worth excluding the possible contamination of extrinsic superconducting phases from the observed superconductivity. The possible extrinsic phases can be well-known binary superconductors consist of Pd and Bi. The binary alloys have different crystal structures with different T_c, namely, monoclinic α-BiPd (space group $P2_1$) with $T_c = 3.8$ K and $\mu_0 H_{c2}(0) = 0.7$ T [36], monoclinic α-Bi_2Pd ($C2/m$) with $T_c = 1.7$ K [37], and tetragonal β-Bi_2Pd ($I4/mmm$) with $T_c = 5.4$ K and $\mu_0 H_{c2}^{ab}(0)$ ($\mu_0 H_{c2}^{c}(0)$) $=$ 1.1 (0.7) T [38]. Since the observed transition temperature in RPdBi does not exceed 1.6 K as shown in Fig. 5 in the main text, we can easily exclude the contamination of monoclinic α-PdBi and tetragonal β-$PdBi_2$ with much higher T_c. On the other hand, T_c of α-Bi_2Pd, rather close to the observed T_c of RPdBi, requires further investigation as described the following paragraph.

To have a closer look at the superconducting properties of α-Bi_2Pd, we present the resistivity of single crystals obtained from flux method in Fig. S2a. Resistivity shows metallic behavior on cooling, followed by the superconducting transition at 1.3 K, slightly lower than the reported T_c [37]. The superconductivity is strongly suppressed by magnetic field, and the critical field obtained from the resistive transition is approximately 300 Oe along out-of- and in-plane orientations at 400 mK (Fig. S2b). The extremely small critical field in monoclinic α-Bi_2Pd is strongly suggestive of inconsistency with the observed $\mu_0 H_{c2}$ of $\sim$3 T for YPdBi and LuPdBi and $\sim$0.5 T for DyPdBi.

The discrepancy of the transition temperature and critical field indicates the observed superconductivity in RPdBi is intrinsic, not due to the contamination of Pd-Bi superconducting alloys. Besides, we note that amorphous Bi undergoes superconductivity at $T_c = 6$ K [37], also inconsistent with the observed T_c in RPdBi. Interestingly, heat treatments at ~ 200°C induce surface superconductivity with T_c of 1.6 K in all RPdBi, independent of the de Gennes factor, which cannot be explained by the formation of a secondary phase and may be correlated with the topological nature.

HEAT CAPACITY

Besides the resistivity and magnetic susceptibility shown in the Fig. 2, low temperature heat capacity also reveals the magnetic transition for RPdBi except for Tm and non-magnetic Y and Lu as shown in Fig. S3. The heat capacity jump at Néel temperature T_N is gigantic, and its magnitude is the order of J/mol K^2, suggesting a huge release of magnetic entropy. Note that upon cooling to 400 mK, the heat capacity for TmPdBi continues to increase, indicating a possible precursor of a magnetic transition below the base temperature of 400 mK. We list the obtained T_N in TABLE S1.

MAGNETIC PROPERTIES

As shown in Fig. 2 in the main text, the temperature dependence of the susceptibility for magnetic rare earth RPdBi shows Curie-Weiss behavior at high temperatures, indicating that the magnetic properties originate from localized $4f$ electron moments. From fitting of the Currie-Weiss law, we obtained the effective moments of $4f$ electrons, μ_{eff}, close to the theoretical ones for respective free R^{3+} ions, μ_{free}, summarize in TABLE S1. The obtained Weiss temperatures Θ_W are negative, consistent with the observed antiferromagnetic orderings in this system.

R	T_N (K)	Θ_W (K)	μ_{eff} (μ_B)	μ_{free} (μ_B)
Sm	3.4	-258	1.9	0.85
Gd	13.2	-49.6	7.66	7.94
Tb	5.1	-28.9	9.79	9.72
Dy	2.7	-14.3	10.58	10.65
Ho	1.9	-9.4	10.6	10.6
Er	1.0	-4.8	9.18	9.58
Tm	<0.4	-1.7	7.32	7.56

TABLE S1: Néel temperature T_N obtained from the heat capacity and magnetization, Weiss temperature Θ_W, and the effective moments μ_{eff} for RPdBi obtained from a fit to the Curie-Weiss expression. The obtained effective moments are close to the free ion moments μ_{free} except for Sm.

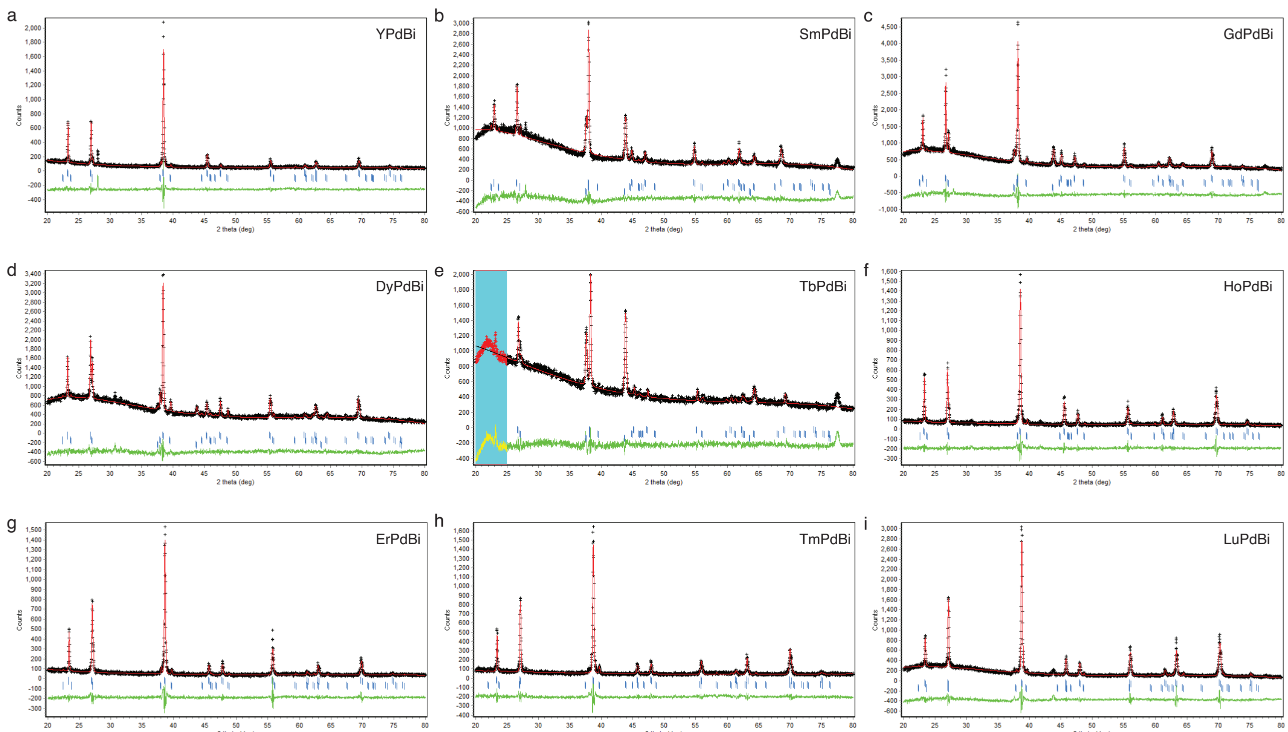

FIG. S1: **X ray diffraction patterns for RPdBi with Cu $K\alpha$ radiation.** Cross symbols are observed data, and lines are theoretical calculations. Upper markers and lower makers correspond to reflections for RPdBi and for elemental Bi. For Sm, Gd, Dy, and Tb, we used two different Bi with $R\bar{3}m$ (middle markers) and $Fm\bar{3}m$ (bottom markers) for the refinements.

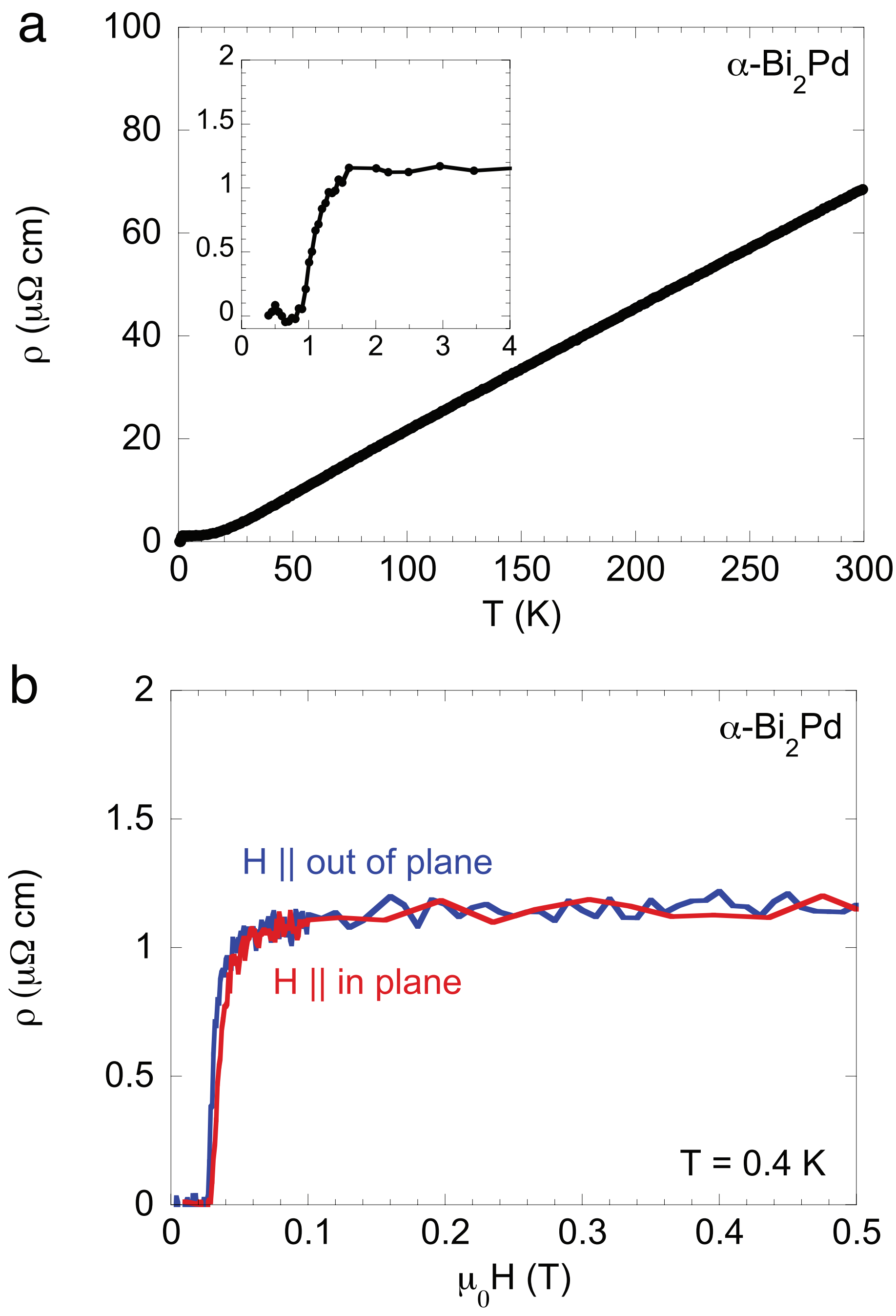

FIG. S2: **Transport properties of $PdBi_2$.** **a**, Resistivity as a function of temperature for $PdBi_2$. Inset: low temperature part of the resistivity. **b**, Field dependence of resistivity.

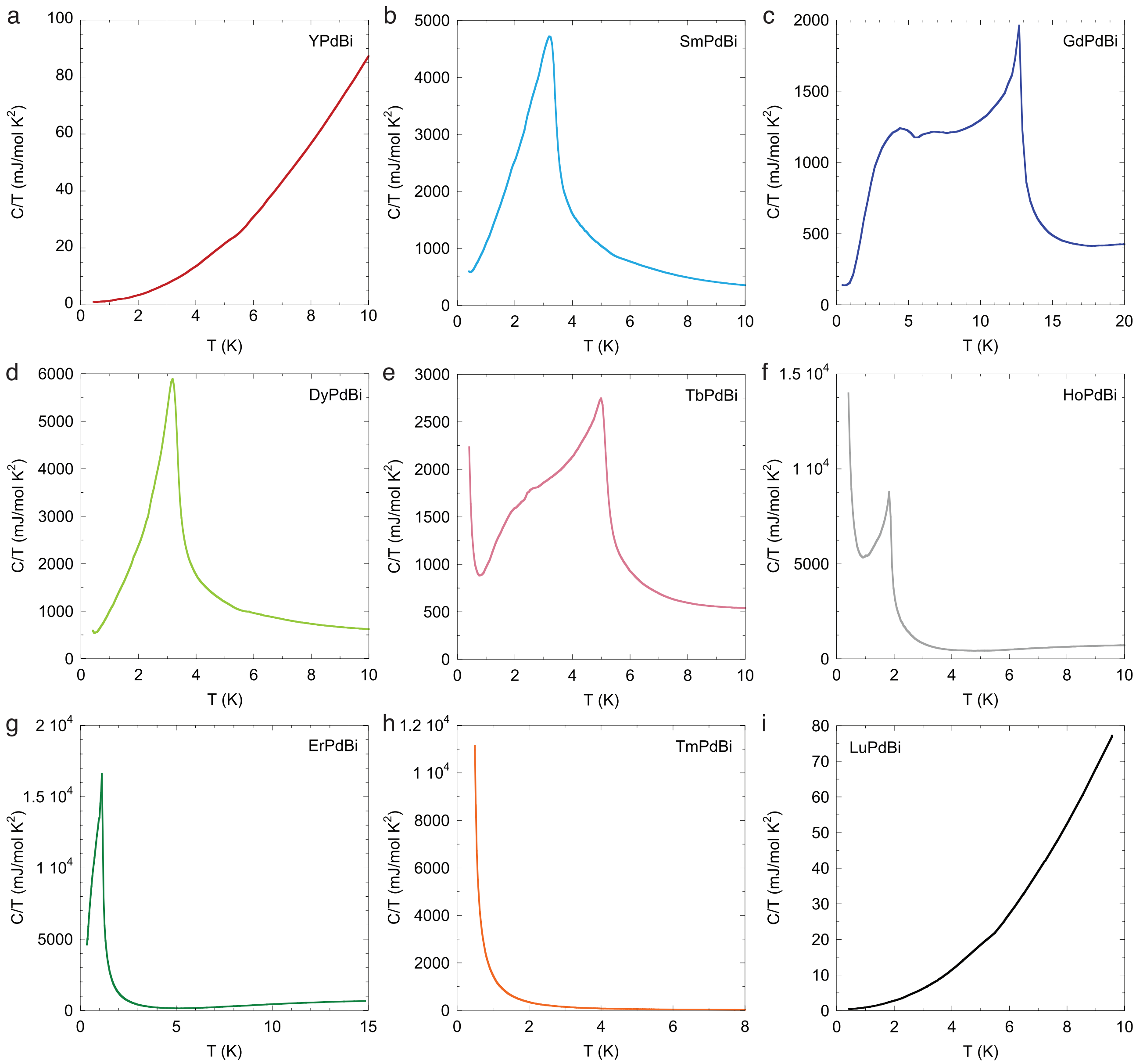

FIG. S3: **Specific heat as a function of temperature for *R*PdBi.** Except for non-magnetic Y and Lu, *R*PdBi undergo antiferromagnetic order at low temperatures. The steep increase in the heat capacity of TmPdBi at low temperatures suggests a possible precursor of magnetic order below 0.4 K.